A SOLUTION FOR IN-SITU SPATIALLY RESOLVED INTENSITY MEASUREMENTS IN BELT FURNACES

Axel Herguth, Christian Derricks, Giso Hahn
University of Konstanz, Department of Physics
PO Box 676, 78457 Konstanz, Germany

ABSTRACT: An intensity tracker has been developed which can be sent through belt furnaces used for thermal treatments that rely on illumination for heating and/or excess charge carrier generation. The device allows for spatially resolved measurements of illumination profiles and can be used to optimize and monitor illumination intensity within the furnaces. The crucial design aspects such as thermal management and the impact of sensor element size on sensitivity are discussed.
Keywords: qualification and testing, in-line intensity measurement, belt furnace, simulation

1 INTRODUCTION

Various types of illuminated belt furnaces are used in industrial production of crystalline silicon solar cells to conduct a variety of in-line heat treatments. For example, this can be the drying of screen-printing pastes in infrared (IR) furnaces, the contact formation at high temperatures in firing furnaces or the regeneration of boron-oxygen related light-induced degradation (BO-LID) or light- and elevated temperature-induced degradation (LeTID) [1-4].

In all these cases, the solar cells or precursors are heated by light which is at least in parts absorbed by the silicon substrate. Even though it is probably irrelevant for drying and firing that excess charge carriers are generated, the typically used incandescent lamps emit a blackbody-like spectrum that extends to energies above the band gap of silicon simply because power emission P per unit area A is linked to filament temperature T via Stefan-Boltzmann's law ($P \sim A \cdot T^4$) and it is in most cases economically more advisable to obtain a required power by increasing temperature than by enlarging area. But rising temperature then implies a spectral shift according to Wien's displacement law ($\lambda_{max} \sim T^{-1}$) towards higher energy photons. For the regeneration of BO-LID and LeTID, excess charge carrier generation is an essential prerequisite anyway. Hence, all of these furnaces employ illumination that leads to excess charge carrier generation.

In all cases it is of vital interest to obtain a spatially homogeneous illumination no matter whether heating or excess charge carrier generation is the aim to guarantee for optimal functionality. However, measuring illumination intensity within a belt furnace, in some cases several meters in length, is not straightforward. Within this contribution we present a patent pending intensity tracker that can be sent through the belt furnace like a solar cell.

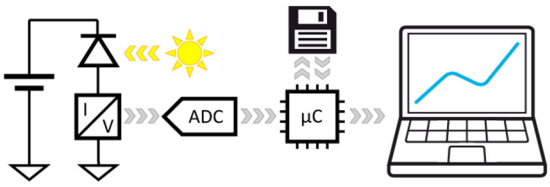

Figure 1: Working principle of the intensity tracker, consisting of sensor element (photosensitive diode, potentially reverse biased), a current-to-voltage converter (I/V), an analog-to-digital converter (ADC), a micro-controller (µC) and memory (disk symbol) temporarily buffering data which then can be transferred to a computer for further processing.

2 DESIGN OF THE INTENSITY TRACKER

The working principle of the intensity tracker is depicted in Fig. 1. It consists of a small solar cell as sensor element providing a current signal that is proportional to the impinging illumination intensity. This current signal is first converted to a voltage signal (I/V converter) which is then digitalized by an analog-to-digital converter (ADC). A microcontroller (µC) queries the ADC's signal in millisecond intervals and buffers the data in memory until it can be transferred to a computer. In certain situations, it can be advantageous to reverse bias the sensor element to improve sensitivity as discussed later on. The entire setup (Fig. 2) is small enough that it can be sent through a belt furnace just like the solar cells being manufactured.

2.1 Heat management

Of course, temperature is a serious issue when sending such a device through a furnace whose core task is to heat solar cells to temperatures above 200°C (regeneration tools) or even 900°C (firing furnaces). Microelectronic devices, even in military grade, are rarely specified to work up to 150°C, if not only up to 80°C. It should be noted as well that common solder joints are limited to temperatures below 200°C. Thus it requires a rigorous heat management which is more restrictive for micro-electronics than for the intensity sensor element itself.

In general, heat management can be done very efficiently by active cooling, however, this requires a heat transfer to a heat sink via a coolant like a gas or a liquid which is maybe not the best idea to be sent through a furnace. Thus passive cooling strategies are the means of

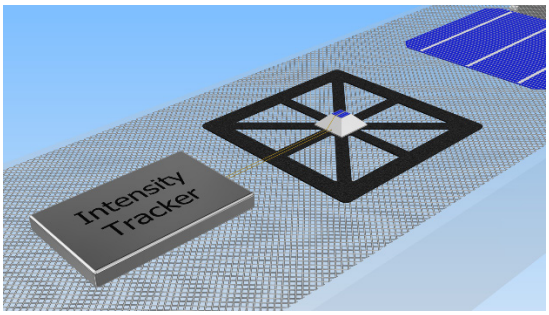

Figure 2: Sketch of the intensity tracker as it travels on the belt though the belt furnace together with a 6" solar cell. The tracker consists of a small solar cell as sensor element mounted on a pyramidal heat sink placed on a carrier plate. The sensor is flexibly connected to a thermally shielded signal processing unit.

choice. In this context, passive cooling has to be understood to mean measures that prevent excessive heating. These can be strategies that simply reduce heat absorption in the first place, improve heat transfer to the surroundings and temporarily buffer heat. In concrete terms, placing the sensor element on a heat sink with high thermal inertia simply due to its comparably large mass slows down heating of the sensor itself; the larger its volume the more it slows down heating. However, this measure is in parts counteracted because a larger volume comes at the price of more surface being exposed to the illumination responsible for the heating and the heat of the surroundings. Here, the first strategy comes into play: reduce absorption of heat in the first place. Even though this is not possible for the sensor element itself as its core task is to measure the impinging light intensity, the residual surfaces of the heat sink can be chosen as mirrors reflecting a large portion of incoming light intensity in the visual and infrared part of the spectrum. Of course, it has to be ensured that light reflected here does not impinge on the sensor element otherwise disturbing the measurement. The chosen pyramidal-shaped heat sink comes with a comparatively large thermal mass while it effectively suppresses reflection towards the sensor element.

More or less the same accounts for the micro-electronics as well, only that temperature restrictions are stricter, and that microelectronics have to be shielded from direct exposure to intense illumination. Hence shielding them in a massive case with reflective surfaces is essential.

2.2 Signal management

Regarding the sensor element, it should be noted that the solar cells normally traveling through the furnace are designed to optimally trap light, and that the illumination within the furnace is typically not designed to provide perpendicular impingement of photons. Hence, the best sensor element available to quantify the intensity (at least above the band gap) absorbed by the solar cell is a solar cell with comparable optical properties as sensor element. However, taking illumination intensities of 10 suns (used for regeneration) to more than 100 suns (used for firing) into account, it is unwise to simply use a solar cell from nowadays mass production with an area of $15.6 \times 15.6\ \mathrm{cm}^2$ as sensor element, because already at 1 sun light intensity a short circuit current I_{sc} of roughly 10 A is generated. Hence, at least at first glance, the current I to be measured would virtually explode to unmanageable 100 A or even 1000 A which also implies massive resistive losses $P = R_{ext} \cdot I^2$ dissipating at any external resistive element R_{ext} in between cell and current-to-voltage converter as well as at its internal resistance.

At second glance, the extracted current I of a solar cell would never increase that much simply because such a current implies a voltage drop $V = R_{ext} \cdot I$ and, as a solar cell is a limited power source, actually extracted current of a solar cell depends on its voltage. In a simple picture, voltage V and extracted current I are linked to each other via the ideal 1-diode-model

$$I(V) = I_{sc} - I_0 \cdot \left[\exp\left(\frac{qV}{kT}\right) - 1\right] \qquad (1)$$

where

$$I_{\mathrm{sc}}(n\ \mathrm{suns}) = n \cdot I_{\mathrm{sc}}(1\ \mathrm{sun}) \qquad (2)$$

represents the light generated current for ideal short-circuit conditions ($V = 0$) at n suns illumination intensity. As the illumination within the furnaces typically differs from the STC's AM 1.5g spectrum [5], it should be noted here that 1 sun refers to an intensity/photon flux of the respective spectrum that yields the same I_{sc} as obtained using the AM 1.5g spectrum [6]. The second term in Eq. 2 corresponds to recombination losses which occur for non-vanishing voltage ($V > 0$). Hence, extracted current and operating voltage V_{op} follow from the relation

$$I(V_{\mathrm{op}}) = \frac{V_{\mathrm{op}}}{R_{\mathrm{ext}}} = I_{sc} - I_0 \cdot \left[\exp\left(\frac{qV_{\mathrm{op}}}{kT}\right) - 1\right] \qquad (3)$$

and depend on the value of the external resistance R_{ext} which 'short-circuits' the solar cell. If that resistance is comparatively small, implying that operating voltage V_{op} is close to zero and thus recombination losses are negligible, more or less all the current leaves the cell ($I \approx I_{sc}$). However, if the external resistance increases, implying a non-negligible operating voltage and thus non-negligible recombination losses, extracted current begins to drop ($I < I_{sc}$). In the extreme case, operating voltage approaches open-circuit conditions and extracted current virtually vanishes: the sensor loses its sensitivity.

As the voltage drop across the external resistance increases linearly with extracted current ($V_{op} = R_{ext} \cdot I$), but open-circuit voltage V_{oc} of a solar cell increases only logarithmically (Eq. 1: $I(V_{oc}) = 0$), the gap between V_{op} and V_{oc} narrows with increasing intensities. Hence, a partial drop in extracted current with increasing intensity becomes more likely, or in other words, extracted current

$$I(n\ suns) \leq n \cdot I(1\ sun) \qquad (4)$$

behaves non-linearly with intensity even though ideal short-circuit current I_{sc} does (Eq. 2).

In reality, the situation is more complex, because the solar cell sensor itself has resistive elements (emitter, metal-to-silicon contact, fingers, busbar) as well contributing to its distributed series resistance. That implies that even if the sensor element's local current density j_{local} follows the 1-diode-model (cp. Eq. 1), current flow within the sensor results in voltage differences dV within the sensor so that local voltage V_{local} corresponds to

$$V_{\mathrm{local}} = V_{\mathrm{op}} + dV \geq V_{\mathrm{op}} \qquad (5)$$

and extracted current corresponds to

$$I(V_{\mathrm{op}}) = \iint j_{\mathrm{local}}(V_{\mathrm{local}})\, dx\, dy \qquad (6)$$

Analogous to the discussion above, an increase in local voltage implies more recombination, and in consequence, less local current density contributes to extracted current. This is exemplarily shown in Fig. 3 for a $5 \times 5\ \mathrm{cm}^2$ solar cell illuminated with 10 suns and short-circuited with $R_{ext} = 100\ \mathrm{m\Omega}$.

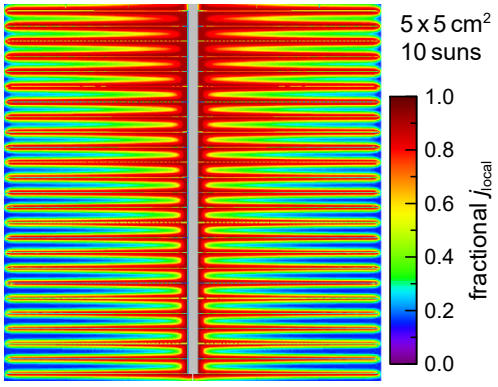

Figure 3: Simulated map of the fraction of extracted local current density for a $5 \times 5\ \mathrm{cm}^2$ solar cell illuminated with 10 suns. Current is extracted at the top end of the tabbed busbar (gray). Calculation done using Griddler 2.5 [7].

The high extracted current of ~5 A of this comparatively large solar cell sensor results in an already high operating voltage V_{op} of 516 mV (V_{oc} ~ 720 mV). The current flow to the extraction point at the upper busbar edge results in local voltages V_{local} well above V_{op} especially in between the fingers further down the busbar (towards the bottom of Fig. 3) due to the high emitter sheet resistance of 75 Ω/sq. In consequence, large parts of the solar cell sensor virtually stop contributing to the extracted current which would be ~10 A otherwise. Thus ignoring this effect, one would erroneously conclude that intensity is apparently rather 5 suns than 10 suns.

Figure 4 shows the I(V) curves of solar cell sensors of different size when subjected to various illumination intensities demonstrating how strongly both, sensor size and illumination intensity, impact sensor functionality. The sensor's internal distributed series resistance strongly distorts the IV curves; the higher the intensity; the stronger the distortion.

Figure 4 depicts the operating points for R_{ext} = 100 mΩ as well. For the 1 × 1 cm² sensor, the comparatively small extracted current results in quite low operating voltages in a range where the IV-curves are more or less not impacted by series resistance. At least in the depicted intensity range, this sensor element behaves linearly with increasing intensity as shown in Fig. 5. For larger sensor sizes, the distorted regime extends more and more to smaller voltages while the operating point shifts steadily upwards well into the distorted regime. In consequence, current is only partly extracted and the sensor element begins to behave non-linearly with increasing intensities.

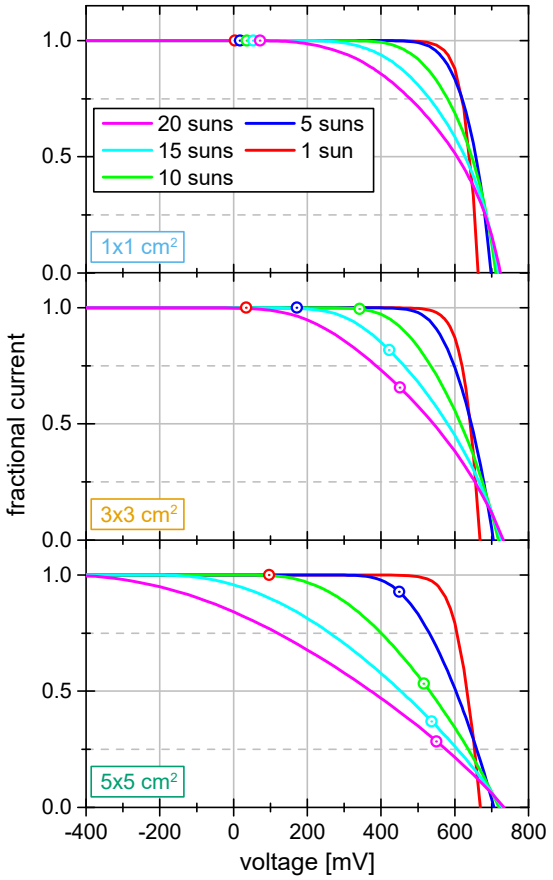

Figure 4: Normalized current-voltage curves for various sensor sizes and intensities. The marked operating points relate to short-circuiting the sensor with R_{ext} = 100 mΩ.

Based on Fig. 4, Figure 5 demonstrates how strongly the onset of non-linearity depends on sensor size and illumination intensity. While the 5 × 5 cm² solar cell sensor becomes insensitive already at ~5 suns, the 3 × 3 cm² sensor element can be used up to ~10 suns. Only the 1 × 1 cm² sensor element allows for measurements in the whole depicted range up to 20 suns. However, somewhere beyond that it becomes non-linear as well.

Even reducing the external resistance R_{ext} in order to push the operating point towards lower voltages in Fig. 4 would not necessarily improve the situation for large sensor sizes illuminated with high intensities because the distortion already extends to negative voltages and even perfectly short-circuiting the sensor (V_{op} = 0) would not result in full current extraction.

In general, the better countermeasure is to negatively bias the sensor element as it pushes the operating point towards lower voltages without the need to excessively reduce R_{ext}. This is exemplarily depicted in Fig. 5 for a bias of -250 mV demonstrating that the onset of non-linearity can be pushed towards higher intensities. However, the downside of biasing the sensor element is that it requires a power source/battery that has to be integrated into the intensity tracker as well. Whereas the required voltage is rather low, the power source/battery has to be capable of providing at least a peak current matching that of the solar cell sensor. While it is easily possible to find such a small power source/battery for a 1 × 1 cm² solar cell sensor where current even at 20 suns rises only to ~0.8 A, it probably becomes problematic for a 5 × 5 cm² solar cell sensor, where current rises to ~20 A for an illumination intensity of 20 suns.

In summary, it is advisable to use a rather small solar cell as sensor element, that can be used without biasing if the external resistance R_{ext} can be kept small enough, *e.g.*, 100 mΩ in the shown example. Then, a 1 × 1 cm² solar cell sensor allows for intensity measurements up to ~20 suns without biasing. If R_{ext} or intensities to be expected are considerably higher, biasing such a small sensor element is probably easier than biasing a larger one. In addition, it should be kept in mind that a power $P = R_{ext} \cdot I^2$ is dissipated at R_{ext} in a probably hot environment where giving off that heat, *e.g.*, by convective cooling, is not that easy anymore.

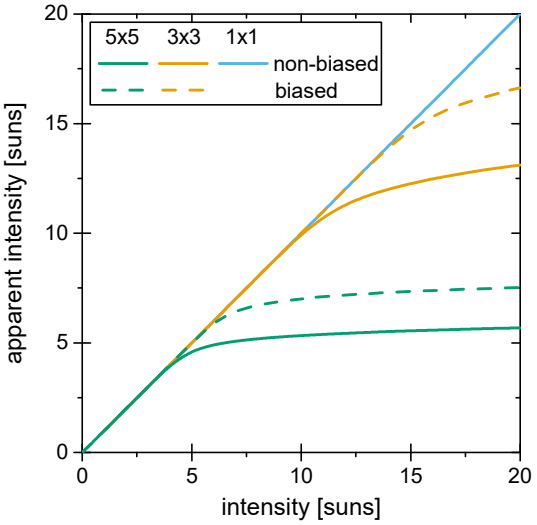

Figure 5: Calculated apparent intensity $I(n \text{ suns})/I(1 \text{ sun})$ (Eq. 4) versus applied intensity (Eq. 3) for different sensor sizes with and without biasing the sensor with -250 mV.

3 APPLICATION EXAMPLE

As mentioned above, optimizing illumination regarding its spatially homogeneous distribution is especially important for tools used for regeneration of BO-LID. Figure 6 shows exemplary measurements of intensity and sensor temperature, respectively, in a *c.reg* tool from *centrotherm international AG*. The tool uses a multitude of halogen lamps spread across three zones whose illumination level (in %) can be adjusted by the user. Due to its small size, the sensor reveals a fluctuation of illumination in belt direction (top graph).

As can be seen from the bottom graph, the temperature of the sensor cell shows the expected upward trend due to thermal buffering but remains comparatively cool even though a 'normal' non-buffered solar cell gets much hotter under these conditions. For example, the 100% setting results in peak temperatures up to almost 350°C for solar cells, while the temperature of the sensor cell did only reach 105°C, a safe regime for solder joints.

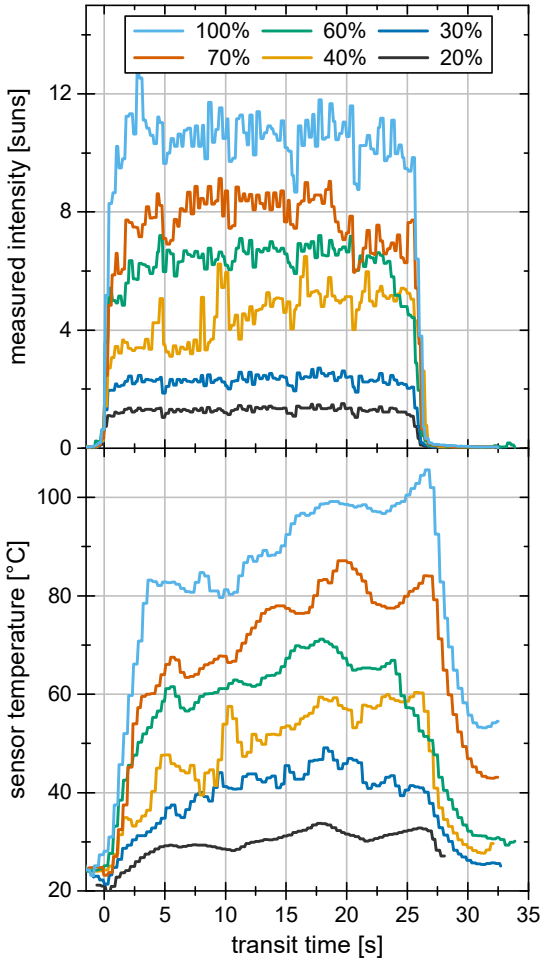

Figure 6: Exemplary measurement of illumination intensity during the transit through a regeneration tool (top) and the temperature of the sensor element (bottom).

ACKNOWLEDGEMENT

Part of this work was supported by the German Federal Ministry of Economic Affairs and Energy under contract numbers 0325877C and 0324001.

The content is the responsibility of the authors.

REFERENCES

[1] D.C. Walter, T. Pernau, J. Schmidt, Proceedings 32nd European Photovoltaic Solar Energy Conference, (2002) 469.

[2] A.A. Brand, K. Krauß, P. Wild, S. Schörner, S. Gutscher, S. Roder, S. Rein, J. Nekarda, Proceedings 33rd European Photovoltaic Solar Energy Conference, (2017) 382.

[3] K.Y. Yen, J.R. Huang, Y.F. Lin, S. Su, S.H.T. Chen, L.W. Cheng, Proceedings 32nd European Photovoltaic Solar Energy Conference, (2016) 495.

[4] https://www.despatch.com/safire.aspx

[5] International Electrotechnical Commission. IEC 60904-3: PV devices – Part 3: Measurement principles for terrestrial photovoltaic (PV) devices with reference spectral irradiance data.

[6] A. Herguth, Energy Procedia, Vol. 124 (2017) 53.

[7] Griddler ver. 2.5, Solar Energy Research Institute of Singapore (SERIS). http://www.griddlersolar.com/